Trunk sap rot of Japanese cedar (*Cryptomeria japonica*) caused by *Fomitiporella sinica*

Masato Torii [a,*], Yu Ichihara [b], Hayato Masuya [a], Tsutomu Hattori [c]

[a] Department of Mushroom Science and Forest Microbiology, Forestry and Forest Products Research Institute, Ibaraki, Japan

[b] Kansai Research Center, Forestry and Forest Products Research Institute, Kyoto, Japan

[c] Principal Research Director, Forestry and Forest Products Research Institute, Ibaraki, Japan

[*]Corresponding author. Department of Mushroom Science and Forest Microbiology, Forestry and Forest Products Research Institute, 1 Matsunosato, Tsukuba, Ibaraki 305-8687, Japan.

E-mail address: masatorii@ffpri.affrc.go.jp (M. Torii)

Text (including abstract, references): 20 pages

Number of tables: 1

Number of figures: 3

The English in this document has been checked by at least two professional editors, both native speakers of English. For a certificate, please see:
http://www.textcheck.com/certificate/p6rQrz

Abstract

Trunk rot caused by the wood decay fungus *Fomitiporia torreyae* is a serious disease of Japanese cedar. The rot is characterized by white sap rot with brown zone lines and vertical depressions on the trunk. During our field investigations on this disease, we found another sap rot on Japanese cedar, characterized by white rot with brown zone lines, with or without less obvious depressions on the trunk. The results of phylogenetic analysis of the most frequently isolated fungus from the diseased trees and morphological observation of basidiocarps previously identified as *Fomitiporella umbrinella* showed that both represented *Fomitiporella sinica*. Our inoculation tests using Japanese cedar showed that *F. sinica* caused longer discoloration in sapwood compared with control treatment. Therefore, we concluded that *F. sinica* was the cause of trunk rot on Japanese cedar as reported for *F. torreyae*, but trunk depressions were not obvious in the trees infected with *F. sinica*. Moreover, branch scars were found around the middle of decaying parts of diseased trees infected with *F. sinica*, and infection with this fungus was assumed to occur via dead branches or pruning scars.

Keywords: decay disease, *Fomitiporella umbrinella*, *Fomitiporia torreyae*, wood decay

Introduction

Japanese cedar, *Cryptomeria japonica* (Thunb. ex L.f.) D. Don, is widely planted for timber production and is one of the most important silvicultural tree species in Japan. Decay diseases often result in economic losses of silvicultural living trees, but serious decay diseases in Japanese cedar plantations have not been reported except for trunk rot by *Fomitiporia torreyae* Y.C. Dai & B.K. Cui. This disease was first reported in southern Ibaraki Prefecture (Imazeki 1960) and was later found in Chiba Prefecture (Aoshima et al. 1964). More than 90% of the trees were occasionally affected by this disease at severely damaged stands (Matsubara et al. 2009). This trunk rot is characterized by white sap rot with brown zone lines and vertical depressions on the trunk (Imazeki 1960) (Figures 1A, B, C). In severely damaged trees, the depressions are more than 6 m in length and 5 cm in depth, and decayed wood below the depression is frequently exposed after debarking (Imazeki 1960). As branch scars are always found around the middle of the trunk depression, infection by the fungus causing the decay is assumed to occur via dead branches (Imazeki 1960; Aoshima et al. 1964). In addition, the depressions on the trunk may develop vertically because the causal fungus likely kills cambium along with vertical spread of the decay (Imazeki 1960).

This disease had long been found only in Chiba Prefecture and limited areas of the neighboring Ibaraki Prefecture (Miyuki et al. 2014), although *F. torreyae* was reported to cause dieback of Japanese umbrella pine, *Sciadopitys verticillata* (Thunb. Siebold & Zucc) (Hattori et al. 2012; Ota et al. 2014) and dwarfing of Japanese pear, *Pyrus pyrifolia* var. *culta* (Makino) Nakai in other prefectures (Shiota et al. 2008; Ota et al. 2014; Nakamura 2016). Recently, a similar trunk rot on Japanese cedars was found in Kyoto Prefecture, more than 350 km from Chiba and Ibaraki Prefectures, and the causal fungus

of the decay was also identified as *F. torreyae* based on morphological observations of the basidiocarps produced on diseased trees and phylogenetic analysis of isolates obtained from the decayed wood of diseased trees (Ota et al. 2016). In addition, Ichihara et al. (2021) detected another wood decay fungus, *Fomitiporella umbrinella* (Bres.) Murrill from trunk rot on Japanese cedar trees at the same site, but a relationship between the fungus and the rot had not been examined. During additional field investigations of the decay in this site, we found another serious sap rot on Japanese cedar, characterized by white rot with brown zone lines, with or without less obvious depressions on the trunk.Thus, another serious rot on Japanese cedar except for caused by *F. torreyae* would be present in this site.

This study was performed to identify the causal fungi of trunk rot on Japanese cedar other than *F. torreyae*. To clarify the taxonomic positions of isolates obtained from the rot, we conducted phylogenetic analysis of the isolates and morphological observation of basidiocarps previously identified as *F. umbrinella* collected in Japan. To characterize the decay, we examined the damage and compared the symptoms with those caused by *F. torreyae*. In addition, to evaluate the pathogenicity, these isolates were inoculated onto living Japanese cedar.

Materials and methods

Sampling of diseased trees and observation of damage

Sampling was conducted at the Momoyama Experimental Forest Site, Kansai Research Center, Forestry and Forest Product Research Institute (34°56′26″N, 135°46′21″E) located in Kyoto. We cut 21 diseased standing trees mainly with longitudinal depressions on the trunk between 2012 and 2020. The approximate ranges of age and diameter at

89 breast height of the examined trees were 7–40 years and 10–25 cm, respectively. Among
90 the trees examined, three standing trees showed trunk sap rot and colonization of a decay
91 fungus different from *F. torreyae*. These trees and cultures were examined for decay and
92 to determine the associated fungus.
93 To characterize external symptoms, we examined the above three trees to determine
94 whether there were depressions in the trunk. These trees were cut into logs 20-cm in
95 length and were then cut vertically at the center of the decayed area for observation of
96 longitudinal sections. To characterize internal symptoms, we examined the decay
97 characteristics and looked for possible infection routes into the trees, including branch
98 scars and trunk injury at and around the middle of the decayed areas. In addition, the
99 vertical lengths and heights of the decayed parts were measured on photographs using
100 ImageJ software (Schneider et al. 2012).
101
102 ***Isolation and identification***
103 To isolate wood decay fungi from diseased trees, several wood pieces of approximately
104 2 × 2 × 2 mm were excised from fresh-cut surfaces of the decayed wood of each sampling
105 tree using flame-sterilized knives. The wood pieces were placed on potato dextrose agar
106 (PDA; Nissui Pharmaceutical, Tokyo, Japan) with or without 10 μg/L benomyl (Benlate;
107 Sumitomo Chemical, Tokyo, Japan) and then incubated at 20°C for 2 weeks to 1 month.
108 During the incubation period, hyphal tips emerging from the inoculated wood pieces were
109 transferred to fresh PDA for pure culture. The isolated fungi were identified based on the
110 DNA sequence of the internal transcribed spacer (ITS) region of rRNA gene.
111 For molecular identification, genomic DNA was extracted from 2–4-week-old cultures
112 on PDA at 20°C using the DNeasy Plant Mini Kit (Qiagen, Valencia, CA, USA)

according to the manufacturer's instructions. The ITS region was amplified using the primers ITS1F (Garden and Bruns 1993) or ITS5 and ITS4 (White et al. 1990). Polymerase chain reaction (PCR) was performed using 25-μL reaction mixtures containing GoTaq Master Mix (Promega, Madison, WI, USA) according to the manufacturer's instructions. PCR consisted of an initial denaturation step at 95°C for 2 min, followed by 35 cycles of 95°C for 1 min, 56°C for 30 s, and 72°C for 1 min, with a final extension at 72°C for 5 min. The resulting PCR products were purified using ExoSAP-IT (Thermo Fisher Scientific, Waltham, MA, USA). Direct sequencing of the PCR products was performed using the same primers as described above with the Big Dye Terminator v. 3.1 cycle sequencing kit (Applied Biosystems, Foster City, CA, USA). Purified products were analyzed on the ABI 3130xl Genetic Analyzer (Applied Biosystems). As some sequencing results included ambiguous base calls possibly because of heterozygosity, these PCR products were cloned using the pGEM-T Easy Vector System (Promega). At least three transformed clones per isolate were amplified and sequenced as described above. Sequences were assembled and edited using MEGA X (Kumar et al. 2018) and were deposited in the DDBJ with accession nos. LC662769–LC662790 (Table 1).

Based on the results of BLASTn search (Altschul et al. 1997) using the sequences analyzed in this study, most isolates of wood decay fungi obtained from the trunk rot were determined to be a *Fomitiporella* sp. Therefore, phylogenetic analysis was performed using select sequencing data from *Fomitiporella* spp. and their allied taxa based on Salvador-Montoya et al. (2020), as well as those from isolates from the trunk rot. Moreover, we also included newly analyzed sequences of isolates from basidiocarps previously identified as *F. umbrinella* (= *Phellinus umbrinellus* (Bres.) Ryv.) collected in

Japan, i.e. Kyoto, Kagoshima and Okinawa Prefectures and Bonin Islands (Table 1). In the analysis, *Inocutis dryophila* was used as an outgroup according to Salvador-Montoya et al. (2020). Sequences were aligned using the online version of MAFFT 7 with the E-INS-i options (Katoh et al. 2019). The sequence alignment was deposited in TreeBASE (ID: S29135). Phylogenetic trees were inferred by maximum likelihood analysis using MEGA X. Alignment gaps and missing data were eliminated from the alignment data using the complete deletion option, and 1000 bootstrap replicates were performed. The most appropriate nucleotide substitution model was determined in MEGA X using the model selection option.

Morphological observations

To clarify the taxonomic position of the *Fomitiporella* sp., morphological characteristics of the type specimen of *Fomitiporella sinica* Y.C. Dai, X.H. Ji & Vlasák were compared with specimens previously identified as *F. umbrinella* collected in Japan. All Japanese specimens were deposited at the Mycological Herbarium of the Forestry and Forest Products Research Institute (TFM), Japan (Table 1). Microscopic examination was conducted on freehand sections of specimens mounted in water, 5% (w/v) KOH solution, 1% (w/v) phloxine solution, Melzer's reagent, and Cotton Blue. Spore measurements (n = 40 per specimen) were made in KOH. The following abbreviations were used: IKI−, neither amyloid nor dextrinoid stained with Melzer's reagent; CB(+), cyanophilic after 12 h of staining with Cotton Blue; Q, spore length/width ratio; Q_m, mean Q; L_m, mean spore length; W_m, mean spore width.

Evaluation of pathogenicity

We conducted inoculation tests to evaluate the pathogenicity of the *Fomitiporella* sp. isolated from the decay on Japanese cedar. Two isolates (FFPRI421038 and FFPRI421039) (Table 1) were inoculated onto three Japanese cedar trees (ca. 20 years old, 9.5 m in height, 12 cm in diameter at breast height) at the nursery of the Forestry and Forest Product Research Institute (36°00′30″N, 140°07′54″E) on 30 Jul 2020. In addition, one *F. torreyae* isolate (FFPRI421024), which was isolated from decayed wood of Japanese cedar in Ibaraki Prefecture, was also used for the inoculation test. Japanese beech (*Fagus crenata*) sapwood dowels, 18 mm in length and 9 mm in diameter, were sterilized in distilled water at 121°C for 15 min. The dowels were then co-incubated with each isolate for 3 months on sawdust rice bran medium, which consisted of 25 g Japanese beech sawdust, 5 g rice bran, and 70 g distilled water. Incubated dowels were used as inocula for the inoculation test. We bored four holes, 18 mm in depth and 10 mm in diameter, on the stem of each test tree at a height of approximately 150 cm above the ground using a surface-sterilized hand drill. Inocula of the three isolates and a sterilized dowel as a control were inserted into the holes on each test tree. Thus, four treatments, i.e., inoculation of the three isolates and control, were conducted on each tree.

Inoculated trees were cut down on 30 Jun 2021, approximately 48 weeks after inoculation. Logs approximately 40 cm in length were collected from approximately 20 cm above and below the inoculation points and cut vertically at each inoculation point. Each longitudinal section was photographed, and the lengths of discolored sapwood above and below the inoculation points were measured on the photographs using ImageJ. The lengths were defined as the distances from the upper or lower tips of the discolored areas to the edges of the inoculation holes. The average length of the upper and lower sides from each hole was used for evaluation. Fungal re-isolation was conducted from

discolored sapwood near each inoculation point in the same manner as described above for isolation from diseased trees.

Pairwise comparisons of the lengths between each isolate and the control were conducted by the Mann–Whitney U-test. Statistical analyses were performed using R v. 4.0.4 (R Core Team 2021).

Results

Molecular phylogenetic analysis

Based on the results of BLASTn search to infer the closest taxa, *Fomitiporella* sp. was the species most frequently isolated from the decayed wood of all sampled trees, and another wood decay fungus, *Amylostereum orientale* S.H. He & Hai J. Li, was occasionally isolated from one sampled tree (data not shown). From the newly analyzed sequences in this study, two representative sequences were chosen for phylogenetic analysis. Our isolates obtained from both decayed wood of Japanese cedar and *Fomitiporella* basidiocarps collected in Japan formed a strongly supported clade with sequences of *F. sinica* described in China (Figure 2). In addition, three phylogenetic lineages within *Fomitiporella* species described by Salvador-Montoya et al. (2020), i.e. *Fomitiporella* s.s., Clade I and II, were resolved. Consequently, we concluded that *F. sinica* is the correct name to represent the fungus precisely identified as *F. umbrinella* (as *P. umbrinellus*) in Japan.

Taxonomy

Fomitiporella sinica Y.C. Dai, X.H. Ji & Vlasák, Mycologia 109: 317. 2017

Basidiocarps perennial, resupinate. Poroid surface rust-brown to dull brown, more or less glancing and occasionally cracked when dry. Pores angular, 5–8 per mm. Tubes stratified, each layer up to 2.5 mm deep. Hyphal system dimitic. Generative hyphae hyaline, thin- to thick-walled, occasionally branched, frequently septate. Skeletal hyphae dominant, thick-walled, unbranched, aseptate. Setae absent. Cystidia and cystidioles absent. Rhomboid crystals variably present according to specimen, sparse or abundant. Basidiospores broadly ellipsoid, thick-walled, smooth, yellowish-brown in water, becoming chestnut to ferruginous in KOH, IKI−, CB(+), 3.5–4.5 × 2.5–3.5 μm based on seven specimens (n = 280) including the holotype, range of $L_m \times W_m$ = 4.0–4.3 × 2.8–3.0 μm, L_m = 4.1 μm, W_m = 2.9 μm, Q = 1.18–1.70, Q_m = 1.41, Q_m range = 1.35–1.53.

Type of rot: White rot.

Distribution and substrate: Known from warm temperate and subtropical areas of China and Japan. Basidiocarps found mainly on hardwood species (*Casuarina* sp., *Clethra barbinervis* Siebold & Zucc., *Melia* spp., *Rhaphiolepis indica* (L.) Lindl., *Rhododendron* sp.) but also on the conifer *C. japonica* in Japan (specimens not referred here). Based on this and previous phylogenetic analyses (Salvador-Montoya et al. 2020), this fungus also grows on *P. pyrifolia* var. *culta* and the roots of *Erythrorchis altissima* (Blume) Blume.

Specimens examined: CHINA, Jiangxi Prov., Guangzhou, Fenyi County, Dagang Mountain, on dead *Rhododendron* sp., 18 Sep 2008, coll. Y.C. Dai (holotype, BJFC 004710); JAPAN, Kyoto Pref., Kyoto City, Mt. Kodaiji, on hardwood, 25 Oct 2012, Coll. T. Hattori (TH; TFM F-30082); Kyoto City, Matsugasaki, on dead standing *Clethra barbinervis*, 7 Mar 2021, Coll. Y. Ichihara (TFM F-30084); Okinawa Pref., Iriomote Is., Ohmija, on hardwood, 20 Oct 2010, Coll. TH (TFM F-29139); Okinawa Is., Kunigami-

232 gun, Motobu, on living *Melia azedarach*, 11 Dec 2020, Coll. S. Tsujimoto (TFM F-
233 30083); Tokyo Metro., Bonin Islands, Hahajima Is., Nakanotaira, on *Rhaphiolepis indica*,
234 5 Nov 2012, Coll. TH, Y. Ota (YO) and H. Masuya (HM; TFM F-28658); Bonin Islands,
235 Chichijima Is., Kuwanokiyama, on hardwood, 10 Nov 2013, Coll. TH, YO and HM (TFM
236 F-28811).
237
238 ***Disease symptoms***
239 We found sap rot with or without less obvious depressions on the trunks of living Japanese
240 cedars at the site (Figures 1D, E), and all of the associated decay was white rot with brown
241 zone lines (Figure 1F). In addition, we observed branch scars around the middle of the
242 decaying parts, and the scars were often more severely decayed than the surrounding
243 sapwood (Figure 1G). The heights of the scars ranged from 2.4 to 7.3 m above the ground.
244 The vertical lengths of the decaying parts of the three sampled trees ranged from 0.6 to
245 2.4 m.
246
247 ***Pathogenicity***
248 Inoculated fungi were not re-isolated from one inoculated part with FFPRI421038 (*F.*
249 *sinica*) and one with FFPRI421024 (*F. torreyae*). These data were excluded from
250 subsequent analyses. In addition, another wood decay fungus, *Peniophora* sp., was
251 isolated from one inoculated part in the control treatment, and the discoloration length
252 was 60 mm. Although we have no information about the pathogenicity of *Peniophora* sp.
253 on Japanese cedar, the data were excluded from the analyses to ensure reliable results.
254 We did not find decayed areas on all of the inoculated trees but did observe discoloration

around inoculation holes on all trees. The lengths of discoloration caused by both of the inoculated fungi were significantly longer than those of the control ($p < 0.05$) (Figure 3).

Discussion

The fungus examined here was first reported as *Poria inermis* Ellis & Everh. (= *Phellinus inermis* (Ellis & Everh.) G. Cunn., *Fomitiporella inermis* (Ellis & Everh.) Murrill) in Japan (Yasuda 1918). However, *P. inermis* has spores measuring 5–6 × 4–4.5 µm and strong host preference for Aquifoliaceae (Gilbertson and Ryvarden 1987), while Yasuda (1918) described the fungus as having smaller spores (4–5 × 3–4 µm), and host preference was not recognized in Japan. Therefore, *Phellinus umbrinellus* (= *Fomitiporella umbrinella*) has long been applied for the Japanese fungus (e.g., Hattori and Hongo 1990; Neda and Hattori 1991; Núñez and Ryvarden 2000). This fungus is often associated with living Japanese pear (Fukuta et al. 2017). Salvador-Montoya et al. (2020) concluded that *F. umbrinella* from Japanese pear as well as one of the mycorrhizal fungi on the climbing orchid *E. altissima* examined by Ogura-Tsujita et al. (2018) represent *F. sinica*, recently described from China, based on comparison of the donated sequencing data. The present study also confirmed that both the isolates from trunk sap rot of living Japanese cedar and several specimens identified as *F. umbrinella* in Japan actually represent *F. sinica*.

Fomitiporella sinica was described based on materials from dead and living angiosperm trees in China, but its pathogenicity in living trees was not noted in the original description (Ji et al. 2017). This fungus is often associated with Japanese pear trees damaged by Japanese pear dwarf disease (Fukuta et al. 2017). Imai and Inubushi (2019), however, concluded that *F. sinica* is not the causal fungus of this disease but may cause distinctive

278 trunk rot on living Japanese pear because, on inoculation tests, its decay length was three
279 times that caused by *F. torreyae*, the causative fungus of Japanese pear dwarf disease.
280 *Fomitiporella sinica* was isolated from most of the decayed parts of all diseased trees
281 examined here. *Amylostereum orientale* (previously reported as *Amylostereum*
282 *laevigatum* (Fr.) Boidin in Japan) was another decay fungus occasionally isolated from
283 one of the diseased trees, but it causes wood discoloration on Japanese cedar and is not a
284 cause of distinctive white rot with brown zone lines and trunk depressions (Tabata and
285 Abe 1997, 1999a). In addition, *A. orientale* (as *A. laevigatum*) has limited decay ability
286 on Japanese cedar (Tabata and Abe 1999b). Therefore, we concluded that *F. sinica* was
287 the cause of the trunk rot on living Japanese cedar examined in this study. In our
288 inoculation tests, the length of the discoloration caused by *F. sinica* isolates was longer
289 than or almost identical to that caused by a *F. torreyae* isolate. Aoshima et al. (1964)
290 reported that the length of depressions on trunks caused by *F. torreyae* was up to 6.0 m,
291 suggesting that the decay length caused by this fungus can be nearly 6.0 m in some cases.
292 Meanwhile, the decay length caused by *F. sinica* in this study was up to 2.5 m, although
293 the number of samples examined in this study was limited. *Fomitiporella sinica* can be
294 another serious trunk rot pathogen on Japanese cedar as reported for *F. torreyae*.
295 The decay symptoms on Japanese cedar caused by *F. sinica* were partly similar to those
296 caused by *F. torreyae*, sharing white rot with brown zone lines on the trunk sapwood
297 (Figures 1A, F) and decay length up to several meters. However, trunk depression was
298 not obvious in the trees infected by *F. sinica* examined in this study, while distinct stem
299 depression above the decayed area is one of the characteristic symptoms caused by *F.*
300 *torreyae*. Stem depression by *F. torreyae* is considered to be due to cambium necrosis
301 following trunk rot below the depression (Imazeki 1960). In the present study, no or only

limited cambium necrosis was observed, and stem depression may not have been produced or may have been limited on the trees infected by *F. sinica*. However, our survey was conducted on limited trees within a single study site, and it is necessary to observe more diseased trees at various sites to define the exact symptoms caused by *F. sinica*.

Trunk rot caused by *F. sinica* may be confused with that caused by *F. torreyae*, especially during the early stages, and may be present in diseased stands infected with the latter because of the similar decay symptoms as indicated above. To evaluate the disease impact by *F. sinica* against timber production of Japanese cedar, it is necessary to re-examine the causal fungus at diseased areas previously identified as *F. torreyae*. Trunk rot of Japanese cedar by *F. torreyae* is often identified not only by the symptoms but also by morphological characteristics of the basidiocarps made on diseased trees and molecular characteristics of the isolates obtained from decayed wood. Identification by the latter two methods can be more accurate, but basidiocarps are produced infrequently on the infected trees, and molecular identification is time consuming. With regard to Japanese pear dwarf disease, selective primers and a multiplex loop-mediated isothermal amplification method were developed for specific detection of *F. torreyae* and *F. sinica* (as *F. umbrinellus*) (Suzuki et al. 2015; Fukuta et al. 2017). Use of this technique may enable accurate and rapid diagnosis of these trunk rots of Japanese cedar.

Branch scars were found around the middle of the decaying parts of diseased trees infected with *F. sinica*. Therefore, infection by the fungus is assumed to occur via dead branches or pruning scars. As our study site was an experimental stand and was not managed regularly for timber production, dead branches would have been more likely routes of infection than pruning scars. In the decay disease caused by *F. torreyae*, the

infection was also assumed to occur via dead branches (Imazeki 1960; Aoshima et al. 1964). In fact, disease occurrence was lower in stands where pruning was performed to prevent and remove dead branches than in stands without pruning (Nakagawa 2000; Matsubara et al. 2009). Therefore, exclusion of possible infection routes can reduce the likelihood of disease occurrence. In this study, the heights of branch scars assumed to be infection routes by *F. sinica* ranged from 2.4 m to 7.3 m above the ground, suggesting that *F. sinica* may spread via basidiospores from infected trees to other trees. Therefore, basidiocarp formation may play an important role in disease spread within stands and to adjacent areas. *Fomitiporella sinica* appears on various hardwoods (Fukuta et al. 2017; Ji et al. 2017), and the basidiocarps in hardwood stands around Japanese cedar stands may act as infection sources. Basidiocarps of *F. torreyae* are rarely found on living Japanese cedar trees but are often observed on the cut and thinned wood residues of diseased trees unattended within stands (Iwasawa and Miyuki 2011). These residues would increase the inoculum mass of *F. torreyae* and the likelihood of disease occurrence. Although we do not have information about the effects of surrounding hardwood stands as sources of basidiospores to cause *Fomitiporella* stem rot on Japanese cedar, stand management to control this disease should include adequate pruning and removal of the diseased wood residues outside the stands.

Acknowledgements

We thank Prof. Y.C. Dai of Institute of Microbiology, Beijing Forestry University for the loan of the holotype of *F. sinica*. We are grateful to Mr. Satoshi Tsujimoto of Okinawa Churashima Foundation for providing samples and the staff of Research Coordination Office of Kansai Research Center, Forestry and Forest Product Research Institute, for

their help during sampling. We also thank Ms. Kazuko Komaru and Atsuko Matsumoto of Forestry and Forest Product Research Institute for their assistance with the molecular experiments.

Disclosure statement

The authors declare no conflicts of interest.

Funding

This study was supported in part by research grants from the Forestry and Forest Products Research Institute, Tsukuba, Ibaraki Prefecture, Japan (#201708 and #202005).

361 **References**

362 Altschul SF, Madden T L, Schaffer AA, Zhang J, Zhang Z, Miller W, Lipman DJ. 1997.
363 Gapped BLAST and PSI-BLAST: a new generation of protein database search
364 programs. Nucleic Acids Res. 25:3389–3402.

365 Aoshima K, Hayashi Y, Yonebayashi H, Kondo H. 1964. Sanbu-sugi no Hi-akagaresei-
366 mizogusare-byo [Trunk rot on Sanbu-sugi]. Trans Jpn For Soc. 75:394–397. Japanese.

367 Fukuta S, Nagai H, Suzuki R, Matsumoto Y, Kato S, Saka N, Horikawa H, Kato S,
368 Miyake N. 2017. Detection of *Fomitiporia torreyae* and *Fulviformes umbrinellus* by
369 multiplex loop-mediated isothermal amplification (mLAMP) for diagnosis of Japanese
370 pear dwarf. Ann Appl Biol. 170:170–178.

371 Garden M, Bruns TD. 1993. ITS primers with enhanced specificity for basidiomycetes –
372 application to the identification of mycorrhizae and rusts. Mol Ecol. 2:113–118.

373 Gilbertson RL, Ryvarden L. 1987. North American polypores. Vol. 2. Oslo: Fungiflora.

374 Hattori T, Hongo T. 1990. Wood-decaying hymenomycetes in Amami Island. Mem Natl
375 Sci Mus. 23:63–67. Japanese.

376 Hattori T, Tanaka M, Kuriu T. 2012. Dieback of *Sciadopitys verticillata* caused by
377 *Fomitiporia* sp. Abstract of annual meeting Forestry Society of Japan. 123:pb053.
378 Japanese.

379 Ichihara Y, Hattori T, Matsunaga T, Takahashi SY. 2021. A survey of trunk rots in stem
380 breakage trees by strong winds in a *Cryptomeria japonica* plantation. For Pests. 70:91–
381 97. Japanese.

382 Imai K, Inubushi Y. 2019. Appearance of fruit body, infection status of stem and
383 possibility participation with Japanese pear dwarf disease by related species of
384 *Fomitiporia torreyae* in orchard having frequently symptoms of Japanese pear dwarf

385 disease in Tokushima prefecture. Bull Tokushima Agric For Fisch Technol Support
386 Cent. 6:27–36. Japanese.
387 Imazeki R. 1960. [A new disease of Sanbu-sugi, “Hi-akagaresei-mizogusare-byo” and its
388 ecological prevention]. For Pest News. 9:240–245. Japanese.
389 Iwasawa M, Miyuki Y. 2011. Fruit bodies formation of Japanese cedar stem sap rot
390 fungus in logging residues. Abstract of annual meeting Forestry Society of Japan.
391 122:D36. Japanese.
392 Ji XH, Vlasák J, Zhou LW, Wu F, Dai YC. 2017. Phylogeny and diversity of
393 *Fomitiporella* (Hymenochaetales, Basidiomycota). Mycologia, 109:308–322.
394 Katoh K, Rozewicki J, Yamada KD. 2019. MAFFT online service: multiple sequence
395 alighment, interactive sequence choice and visualization. Brief Bioinform. 20:1160–
396 1166.
397 Kumar S, Stecher G, Li M, Knyaz C, Tamura K. 2018. MEGA X: molecular evolutionary
398 genetics analysis across computing platforms. Mol Biol Evol. 35:1547–1549.
399 Matsubara I, Ishitani E, Fujibayashi N, Nakagawa S. 2009. Ratio of outbreak of sap rots
400 caused by *Phellinus punctatus* in a Sambu-sugi cryptomeria stand under early and hard
401 pruning. Kanto Shinrin Kenkyu, 60, 215–216. Japanese.
402 Miyuki Y, Terashima Y, Iwasawa M, Fukushima S, Endo R. 2014. Recent findings on
403 white rot of the Japanese cedar stem and the causative agent *Fomitiporia torreyae*. Ann
404 Res Bull Chiba Prefect Agric For Res Cen. 6:125–131. Japanese with English abstract.
405 Nakagawa S. 2000. Preventive effect of “hi-akagaresei-mizogusare-byo” by early
406 pruning. For Pests. 49:204–209. Japanese.
407 Nakamura H. 2016. Diseases of Japanese cedar and Japanese pear caused by *Fomitiporia*
408 *torreyae*. Shinrin Kagaku. 9:240–245. Japanese.

409 Neda H, Hattori T. 1991. Mushroom (basidiomycetes). In: Ono M, Kimura M, Miyashita
410 K, Nagoshi M, editors. Report of the Second General Survey of Natural Environment
411 of the Ogasawara (Bonin) Islands 2. Tokyo: Tokyo Metropolitan University; p. 36–55.
412 Núñez M, Ryvarden L. 2000. East Asian polypores Vol. 1. Oslo: Fungiflora.
413 Ogura-Tsujita Y, Gebauer G, Xu H, Fukasawa Y, Umata H, Tetsuka K, Kubota M,
414 Schweiger JMI, Yamashita S, Maekawa N, et al. 2018. The giant mycoheterotrophic
415 orchid *Erythrorchis altissima* is associated mainly with a divergent set of wood‐
416 decaying fungi. Mol Ecol. 27:1324–1337.
417 Ota Y, Hattori T, Nakamura H, Terashima Y, Lee SS, Miyuki Y, Sotome K. 2014.
418 Taxonomy and phylogenetic position of *Fomitiporia torreyae*, a causal agent of trunk
419 rot on Sanbu-sugi, a cultivar of Japanese cedar (*Cryptomeria japonica*) in Japan.
420 Mycologia. 106:66–76.
421 Ota Y, Kimura KM, Hattori T, Miyuki Y, Endo R. 2016. First reports of trunk rot caused
422 by *Fomitiporia torreyae* in Kyoto prefecture on cultivars of Japanese cedar with no
423 relatedness to ‘Sanbu-sugi’. J For Res. 21:105–109.
424 R Core Team. 2021. R: A language and environment for statistical computing. Vienna: R
425 Foundation for Statistical Computing.
426 Salvador-Montoya CA, Popff OF, Góez-Neto A, Drechsler-Santos ER. 2020. Global
427 phylogenetic and morphological reassessment of *Fomitiporella* s.l. (Hymenochaetales,
428 Basidiomycota): taxonomic delimitation of *Fomitiporella* s.s. and segregation of
429 *Rajchenbergia*, gen. nov. Plant Syst Evol. 306:34.
430 Schneider CA, Rasband WS, Eliceiri KW. 2012. NIH image to ImageJ: 25 years of image
431 analysis. Nat Methods. 9: 671–675.

Shiota A, Kaneko Y, Nakamura H, Yasuda F, Oshida M. 2008. Occurrence of Japanese pear dwarf symptom by Inoculation with *Phellinus* species isolated from diseased trees. Jpn J Phytopathol. 74:37. Japanese.

Suzuki K, Shiota A, Kaneko Y, Suzuki T. 2015. Specific detection of the dwarf Japanese pear pathogen, *Fomitiporia torreyae*, by the polymerase chain reaction. Ann Rep Kanto-Tosan Plant Prot Soc. 62:67–72. Japanese.

Tabata M, Abe Y. 1997. *Amylostereum laevigatum* associated with the Japanese horntail, *Urocerus japonicas*. Mycoscience. 38:421–427.

Tabata M, Abe Y. 1999a. *Amylostereum laevigatum* associated with a horntail, *Urocerus antennatus*. Mycoscience. 40:535–539.

Tabata M, Abe Y. 1999b. Experiments in compulsory oviposition by *Urocerus japonicas* and in wood decay by *Amylostereum laevigatum*. Appl For Sci. 8:203–204. Japanese.

White TJ, Bruns T, Lee S, Taylor JW. 1990. Amplification and direct sequencing of fungal ribosomal RNA genes for phylogenetics. In: Innis MA, Gelfand DH, Sninsky JJ, White TJ, editors. PCR protocols: a guide to methods and applications. New York (NY): Academic Press; p. 315–322.

Yasuda A. 1918. Kinrui-Zakki 79. Bot Mag Tokyo. 381:263–264. Japanese.

450 Table 1. Isolates examined in this study.

Isolate no.	Location	Substrate	Specimen accession no. (TFM F)	Accession no. of ITS sequence
Isolates obtained from diseased trees				
FFPRI421036	Momoyama, Kyoto	decayed wood of *Cryptomeria japonica* 1	-	LC662775, LC662776
FFPRI421038	Momoyama, Kyoto	decayed wood of *Cryptomeria japonica* 2	-	LC662779, LC662780
FFPRI421039	Momoyama, Kyoto	decayed wood of *Cryptomeria japonica* 2	-	LC662781, LC662782
FFPRI421042	Momoyama, Kyoto	decayed wood of *Cryptomeria japonica* 3	-	LC662787, LC662788
Isolates previously identified as *Fomitiporella umbrinella*				
FFPRI421032	Ohmijya, Iriomote Is., Okinawa	basidiocarp on hardwood	29139	LC662769, LC662770
FFPRI421033	Ohsumi, Kagoshima	basidiocarp on hardwood	-	LC662771
FFPRI421034	Mt. Kodaiji, Kyoto	basidiocarp on hardwood	30082	LC662772, LC662773
FFPRI421035	Nakanotaira, Hahajima Is., Tokyo	basidiocarp on *Rhaphiolepis indica*	28658	LC662774
FFPRI421037	Kuwanokiyama, Chichijima Is., Tokyo	basidiocarp on hardwood	28811	LC662777, LC662778
FFPRI421040	Motobu, Okinawa	basidiocarp on *Melia azedarach*	30083	LC662783, LC662784
FFPRI421041	Matsugasaki, Kyoto	basidiocarp on *Clethra barbinervis*	30084	LC662785, LC662786

451

452 **Legends for figures**

453 Figure 1. Representative images of diseased Japanese cedar trees infected with
454 *Fomitiporia torreyae* and *Fomitiporella sinica*. A: White rot with brown zone lines
455 caused by *F. torreyae*. B: Trunk depression caused by *F. torreyae*. C: Trunk depressions
456 on cross-sections of diseased trees by *F. torreyae*. D: Decay without obvious depression
457 on cross-sections of diseased trees infected with *F. sinica*. E: Decay with less depression
458 on cross-sections of diseased trees infected with *F. sinica*. F: White rot with brown zone
459 lines caused by *F. sinica*. G: Branch scar on a longitudinal section around the middle of
460 decaying parts due to *F. sinica*. dw: decayed wood; bs: branch scar. *Bars*: 3 cm.

461

462 Figure 2. Maximum likelihood tree generated from DNA sequences of the ITS region.
463 Bootstrap values (1000 replicates) > 60% are indicated at the branch nodes. Sequences
464 newly analyzed in this study are shown in **bold**.

465

466 Figure 3. Longitudinal lengths of discolored sapwood after inoculation with
467 *Fomitiporella sinica* and *Fomitiporia torreyae* isolates. Values are means ± SD. $N = 4$ for
468 FFPRI421038, FFPRI421024, and control; $n = 5$ for FFPRI421039. FFPRI421038 and
469 FFPRI421039 are *F. sinica*, and FFPRI421024 is *F. torreyae*.

Fig. 1

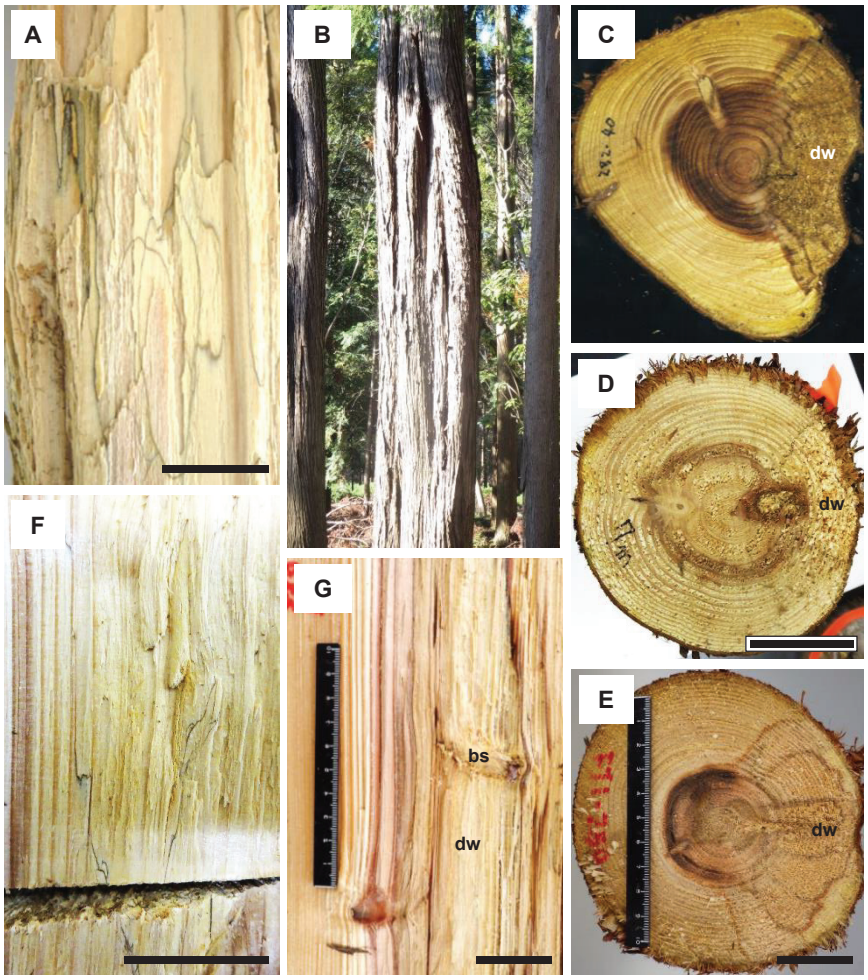

Fig. 2

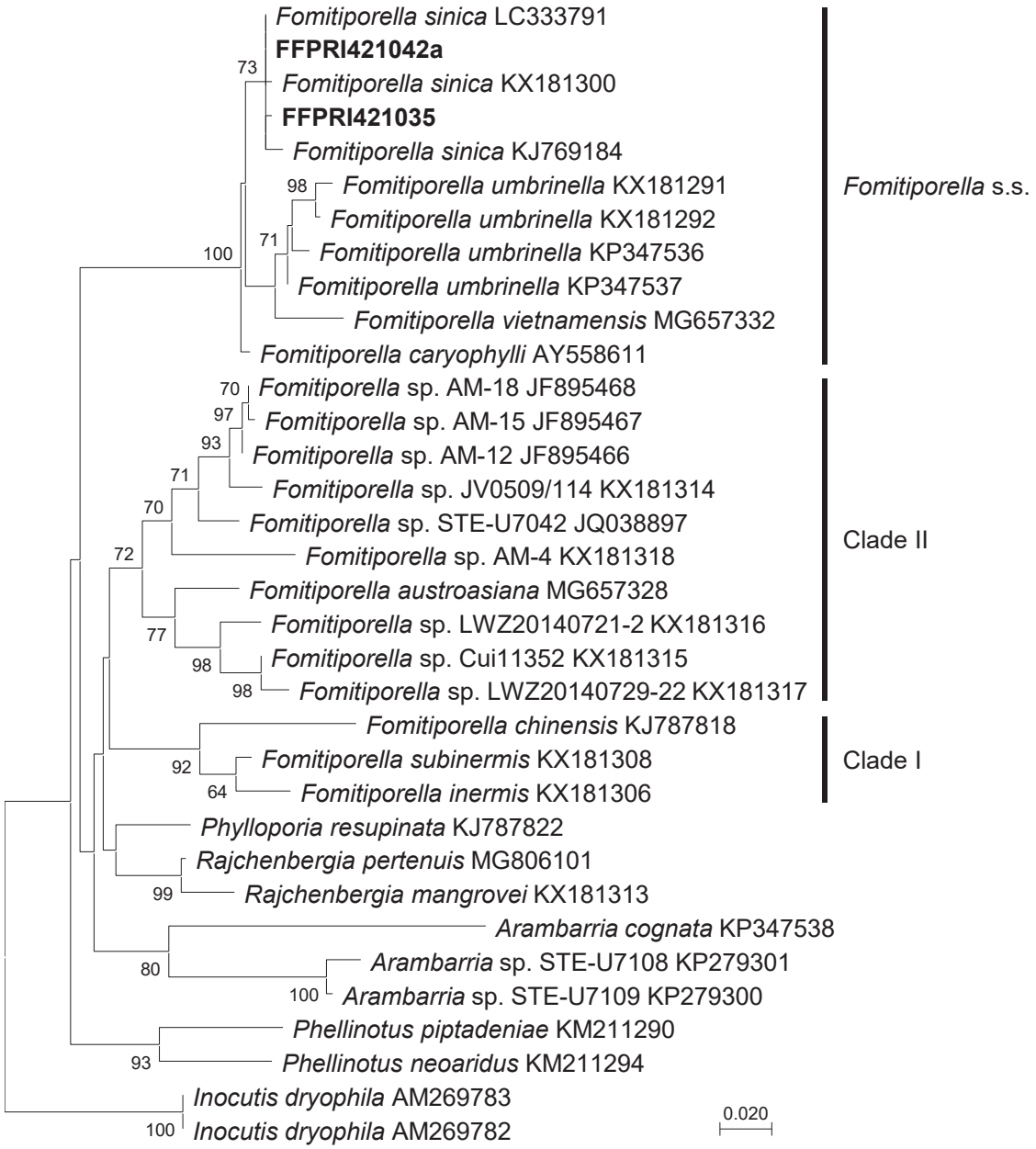
Fomitiporella sinica LC333791
FFPRI421042a
Fomitiporella sinica KX181300
FFPRI421035
Fomitiporella sinica KJ769184
Fomitiporella umbrinella KX181291
Fomitiporella umbrinella KX181292
Fomitiporella umbrinella KP347536
Fomitiporella umbrinella KP347537
Fomitiporella vietnamensis MG657332
Fomitiporella caryophylli AY558611
Fomitiporella sp. AM-18 JF895468
Fomitiporella sp. AM-15 JF895467
Fomitiporella sp. AM-12 JF895466
Fomitiporella sp. JV0509/114 KX181314
Fomitiporella sp. STE-U7042 JQ038897
Fomitiporella sp. AM-4 KX181318
Fomitiporella austroasiana MG657328
Fomitiporella sp. LWZ20140721-2 KX181316
Fomitiporella sp. Cui11352 KX181315
Fomitiporella sp. LWZ20140729-22 KX181317
Fomitiporella chinensis KJ787818
Fomitiporella subinermis KX181308
Fomitiporella inermis KX181306
Phylloporia resupinata KJ787822
Rajchenbergia pertenuis MG806101
Rajchenbergia mangrovei KX181313
Arambarria cognata KP347538
Arambarria sp. STE-U7108 KP279301
Arambarria sp. STE-U7109 KP279300
Phellinotus piptadeniae KM211290
Phellinotus neoaridus KM211294
Inocutis dryophila AM269783
Inocutis dryophila AM269782
73
98
71
100
70
97
93
71
70
72
77
98
98
92
64
99
80
100
93
100
0.020
Fomitiporella s.s.
Clade II
Clade I

Fig. 3

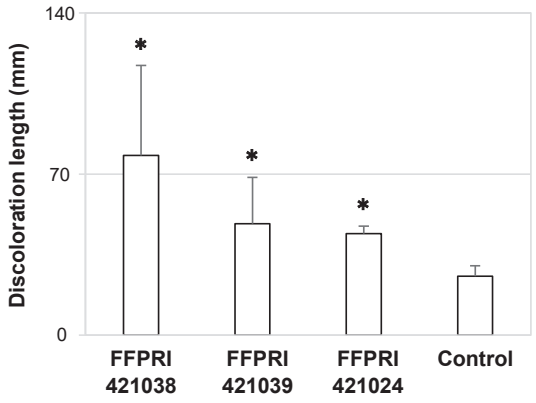
140
70
0
Discoloration length (mm)
*
*
*
FFPRI 421038
FFPRI 421039
FFPRI 421024
Control